Chapter 12
Model-Based Optimal Energy Management Strategies for Hybrid Electric Vehicles

Simona Onori

Abstract Methods from optimal control theory have been used since the past decade to design model-based energy management strategies for hybrid electric vehicles (HEVs). These strategies are usually designed as solutions to a finite-time horizon, constrained optimal control problem that guarantees optimality upon perfect knowledge of the driving cycle. Properly adapted these strategies can be used for real-time implementation (without knowledge of the future driving mission) at the cost of either high (sometime prohibitive) computational burden or high memory requirement to store high-dimensional off-line generated look-up tables. These issues have motivated the research reported in this chapter. We propose to address the optimal energy management problem over an infinite time horizon by formulating the problem as a nonlinear, nonquadratic optimization problem. An analytical supervisory controller is designed that ensures stability, optimality with respect to fuel consumption, ease of implementation in real-time application, fast execution and low control parameter sensitivity. The approach generates a drive cycle independent control law without requiring discounted cost or shortest path stochastic dynamic programming introduced in the prior literature.

12.1 Introduction

In response to the present and future environment and energy challenges worldwide the automotive industry has been focusing on improving vehicle fuel efficiency. Although there is no "silver-bullet" technology to replace the existing ones, at least in the near future, one possible answer to the challenges posed by the automotive and transportation sectors is found in electrification of both the mobility and transport systems. New concepts and new technologies are being developed to realize efficient

S. Onori (✉)
Automotive Engineering Department, Clemson University, Clemson, USA
e-mail: sonori@clemson.edu

H. Waschl et al. (eds.), *Optimization and Optimal Control in Automotive Systems*,
Lecture Notes in Control and Information Sciences 455,
DOI: 10.1007/978-3-319-05371-4_12,

hybrid and electric vehicles suited for both individual and public mobility and for goods distribution in urban areas [7]. This chapter deals with the energy management in HEVs.

12.2 Optimization Problems in HEVs

From a design prospective, a hybrid powertrain is much more complicated than a conventional powertrain as selection hybrid architecture (e.g., series, paralllel, power-split [18]) and component sizing, is not always an easy task because of many design options and the rapidly developing technologies in the automotive industries. Design optimization tools, such as neural networks, genetic algorithms and particle swarm optimization, have been successfully used for powertrain optimization design to maximize fuel economy and minimize emission, weight and cost while guaranteeing vehicle performance (see, for instance, [17], and references therein).

Given a predefined optimized powertrain, a second problem in a HEV is the power split on-board of the vehicle. This is generally referred to as energy management problem or supervisory vehicle control.

Realistic figures of achievable improvement in fuel economy in HEVs range from 10 % for mild hybrids to more 30 % for full hybridized vehicles [10]. This potential can be realized only with a sophisticated control system that optimizes energy flow within the vehicle. The adoption of systematic model-optimization methods using meaningful objective functions has been the pathway to go in order to achieve near-optimal results in designing the vehicle energy management system. In this chapter we focus on *model-based energy management strategy design* techniques. The chapter is organized as follows. In Sect. 12.3 we present a heavy-duty pre-transmission hybrid truck model, which is used as a case study. Section 12.4 presents the standard optimal energy management problem formulation. In Sect.12.5, we review results from the literature to solve the optimal control problem. In the same section, we present the basics of Pontryagin's Minimum Principle (PMP), Equivalent Consumption Minimization Strategy (ECMS) and Adaptive-PMP (A-PMP). Issues related to the real-time implementation of A-PMP are analyzed that motivate the design of a new energy management control framework presented in Sect. 12.6. Section 12.7 reports on some mathematical background used later in Sect. 12.8 where an analytical control law, referred to as nonlinear optimal control strategy (NL-OCS), is presented. Section 12.9 presents a comparison in simulation of the NL-OCS against PMP and A-PMP and the effectiveness of the new control design is shown both from a calibration and implementation standpoint.

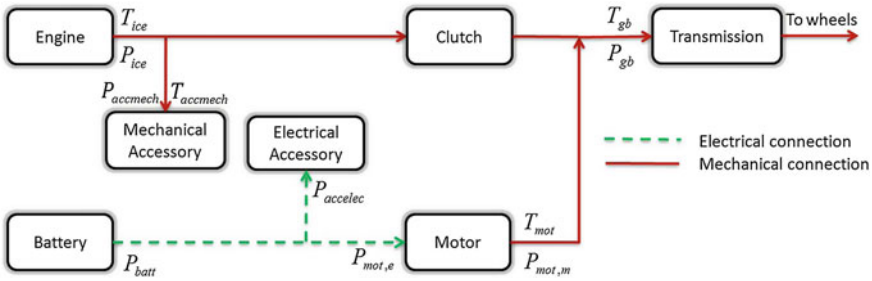

Fig. 12.1 Power flow diagram of pre-transmission parallel HEV

12.3 Case Study: Pre-transmission Parallel Hybrid

A heavy-duty pre-transmission parallel HEV is used as a case study along the chapter. The vehicle architecture and the power flow among the different components (the arrowheads denote the positive power sign convention) are illustrated in Fig. 12.1. The main specifications of the powertrain components are reported in Table 12.1. With the clutch closed, the parallel mode of operation uses both the devices, engine (ice) and motor (mot), to propel the vehicle and their speed is directly determined by the vehicle velocity. The additional degree of freedom available in this mode is used to optimize the vehicle energy usage. The torque/power balance equations are:

$$\begin{cases} T_{mot}(t) + T_{ice}(t) = T_{gb}(t) + T_{accmech}(t), \\ P_{batt}(t) = P_{mot,e}(t) + P_{accelec}(t), \\ \omega_{mot}(t) = \omega_{ice}(t) = \omega_{gb}(t). \end{cases} \tag{12.1}$$

where T_{gb}, ω_{gb} are the instantaneous gearbox torque and speed; T_{mot}, ω_{mot} are the instantaneous electric motor torque and speed; $P_{accelec}$ is the instantaneous electrical accessory power and $P_{mot,e}$ is the instantaneous electrical power at input/output terminals of the electric motor. The battery power (P_{batt}) can be represented as a function of engine power (P_{ice}) and the requested power (P_{req}) as:

$$\begin{cases} P_{batt}(t) = -\frac{1}{\eta_{mot}} P_{ice}(t) + \frac{1}{\eta_{mot}} P_{req}(t), \\ P_{req}(t) = P_{gb}(t) + \frac{1}{\eta_{mot}} P_{accelec}(t) + P_{accmech}(t). \end{cases} \tag{12.2}$$

The vehicle model has been implemented in PSAT (Powertrain Simulation Analysis Toolkit) environment [1].

An analytical model of the engine fuel consumption, based on Willans line approximation is used [10], which expresses the engine chemical power (P_{chem}) as an affine function of the engine power (P_{ice}) and speed (ω_{ice}):

$$P_{chem}(t) = e_0(\omega_{ice}(t)) + e_1(\omega_{ice}(t)) \cdot P_{ice}(t) \tag{12.3}$$

Table 12.1 Vehicle characteristics

Component	Size
Vehicle mass	19,878 kg
Engine capacity	6.7 L Diesel
Engine power	194 kW
Motor power	200 kW
Battery energy capacity	7.5 kWh (27 MJ)
Electrical accessory	7 kW
Mechanical accessory	4 kW

where $P_{chem} = \dot{m}_f \cdot Q_{LHV}$ [Q_{LHV} is the lower heating calorific value of diesel in (kJ/kg)] is the chemical power input to the engine and $P_{ice} = T_{ice}\omega_{ice}$ is the engine power output. The coefficient $e_0(\omega_{ice})$ represents the engine friction losses and $e_1(\omega_{ice})$ the conversion efficiency of the machine. A good approximation of the friction losses and conversion efficiency coefficients is given by expressing e_0 and e_1 as a quadratic fitting with respect to engine speed [25], as:

$$\begin{cases} e_0(\omega_{ice}(t)) = e_{00} + e_{01} \cdot \omega_{ice}(t) + e_{02} \cdot \omega_{ice}^2(t) \\ e_1(\omega_{ice}(t)) = e_{10} + e_{11} \cdot \omega_{ice}(t) + e_{12} \cdot \omega_{ice}^2(t) \end{cases} \tag{12.4}$$

where $e_{ij} > 0$, $i, j = 0, 1, 2$ are the constant Willans line coefficients. Hence, the fuel consumption rate can be written as:

$$\dot{m}_f(t) = \frac{1}{Q_{LHV}}[e_0(\omega_{ice}(t)) + e_1(\omega_{ice}(t)) \cdot P_{ice}(t)] \tag{12.5}$$

or:

$$\dot{m}_f(t) = p_0(\omega_{ice}(t)) + p_1(\omega_{ice}(t))P_{ice}(t) \tag{12.6}$$

with $p_0(\omega_{ice}(t)) = \dfrac{e_0(\omega_{ice}(t))}{Q_{LHV}}$, and $p_1(\omega_{ice}(t)) = \dfrac{e_1(\omega_{ice}(t))}{Q_{LHV}}$.
Note: The Willans line fuel consumption rate model, together with a suitable description of the battery model, is used to reformulate the energy management control problem as an infinite-time horizon optimal problem including stability in Sect. 12.8.

12.4 Problem Formulation

One important characteristic of the energy management problem is that the control objectives are mostly integral in nature (for instance, fuel consumption, emissions per mile of travel, battery life or a combination of the above, [9, 12, 16, 30]), while the control actions are local in time. In addition to that, the control objectives are subject to constraints which are both integral or global, such as maintaining battery

SOC within a prescribed range, and local constraints, such as physical limitation of the actuators. The very nature of this problem has made the task of finding a near-optimal implementable solution a challenging goal motivating a wealth of research over the past decade [23].

12.4.1 Optimal Energy Management Problem in HEVs

In this chapter, we consider the problem of minimizing the total mass of fuel, m_f (g), during a driving mission. This is equivalent to minimizing the following cost J_T:

$$J_T = \int_0^T \dot{m}_f(u(t))dt \tag{12.7}$$

where $\dot{m}_f$ (g/s) is the instantaneous fuel consumption rate, $u(t)$ is the control action, and T is the optimization horizon. The objective function (12.7) is minimized under a set of both local and global constraints, as outlined in the following.

System Dynamics. The system dynamics is given in terms of SOC variation with respect to time according to:

$$\dot{SOC}(t) = -\alpha \frac{I(t)}{Q_{nom}} \tag{12.8}$$

where α represents the Coulombic efficiency [10]; $I(t)$ (A) is the current flowing in (positive) and out (negative) of the battery and Q_{nom} (Ah) is the nominal battery charge capacity. The battery is modeled through the zero-*th* order equivalent circuit model [28], whose parameters are: the equivalent resistance, R_{eq} and the open circuit voltage, V_{oc}. For the application at hand, i.e., charge sustaining HEVs, the battery is used over a range of SOC (typically between 0.5 and 0.8 SOC), where the parameters are not dependent on SOC [28]. Following the discussion in [28] we can express the current $I(t)$ as a function of $P_{batt}(t)$ and write the system dynamics as:

$$\dot{SOC}(t) = -\alpha \frac{V_{oc} - \sqrt{(V_{oc})^2 - 4R_{eq}P_{batt}(t)}}{2R_{eq}Q_{nom}}. \tag{12.9}$$

Global Constraints. In a charge sustaining HEV, the net energy from the battery should be zero over a given driving mission, meaning that the SOC at the end of the driving cycle, $SOC(T)$, should be the same as the SOC at the beginning of the driving cycle, $SOC(0)$, and equal to a reference SOC value, i.e., SOC_{ref}:

$$SOC(T) = SOC(0) = SOC_{ref}. \tag{12.10}$$

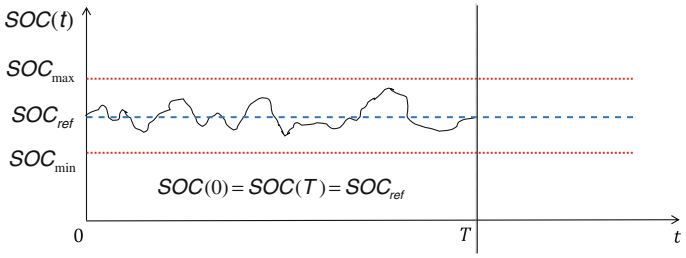

Fig. 12.2 Typical optimal SOC behaviour obtained solving Problem 12.1

Condition (12.10) is justified mainly as a way to compare the results of different solutions by guaranteeing that they start and reach the same level of battery energy. In real vehicles, it is sufficient to keep the SOC between two boundary values.
Local Constraints. Local constraints are imposed on the state and control variables. These constraints mostly concern physical operation limits, such as the maximum engine torque and speed, the motor power, or the battery SOC. For the pre-transmission parallel HEV powertrain local constraints are expressed as:

$$\begin{aligned} P_{batt,min} \leq\ & P_{batt}(t) \leq P_{batt,max}, \\ SOC_{min} \leq\ & SOC(t) \leq SOC_{max}, \\ T_{x,min} \leq\ & T_x(t) \leq T_{x,max}, \\ \omega_{x,min} \leq\ & \omega_x(t) \leq \omega_{x,max},\ x = ice,\ mot. \\ T_{mot,min} \leq\ & T_{mot}(t) \leq T_{mot,max} \end{aligned} \tag{12.11}$$

where the last two inequalities in (12.11) represent limitations on the instantaneous engine and motor torque and speed, respectively; $(\cdot)_{min}, (\cdot)_{max}$ are the minimum and maximum value of power/SOC/torque/speed at each instant. Moreover, at each instant the supevisory controller ensures that the total power request at the wheels is satisfied.

Problem 12.1 The **energy management problem** in a charge sustaining HEV consists in finding the optimal control sequence u^* that minimizes the cost function (12.7) while meeting the dynamic state constraint (12.9), the global state constraint (12.10) and local state and control constraints (12.11).

Problem 12.1 by its very nature is a finite-time horizon (the cost function (12.7) is being minimized over a finite time horizon $[0,\ T]$), constrained (constraints on the state and control are being enforced at each instant of time), nonlinear [the system dynamics (12.9) are nonlinear], nonquadratic (the cost function is the fuel consumption map of the engine), optimal control problem. We refer to Problem 12.1 as the standard HEV energy management problem. A typical SOC behavior resulting from solving Problem 12.1 is shown in Fig. 12.2.

12.5 Finite-Time Horizon Energy Management Strategies

Several approaches have been proposed over the years to solve Problem 12.1. Those can be grouped into [24]:

- non-causal or non-realizable strategies. They require a priori knowledge of the driving cycle and are not applicable in real conditions [e.g., Dynamic Programming (DP), PMP];
- causal or realizable strategies. They do not require a priori knowledge of the driving cycle and are developed with the primary objective of realizability and do not guarantee optimality [e.g., Adaptive-PMP, Stochastic DP, rule-based, equivalent consumption minimization strategy (ECMS)].

Although, the primary objective is to design and implement causal strategies that can be eventually tested on real vehicles, the importance of finding non-causal optimal solutions resides in that: (1) they provide a benchmark solution (global optimum) any causal strategy can be compared against, and (2) properly modified they can be used to develop on-line strategies [27, 28]. In [16], for the first time, and in [4, 5] later, results from DP were analyzed with the aim of gaining insights to generate reproducible rules to design a rule-based strategy capable to mimic the DP behaviour. Although rule-based energy management strategies are relatively easy to develop and implement in a real vehicle, a significant amount of calibration effort is required to guarantee performances within a satisfactory range for any driving cycle. Moreover, rules are not necessarily scalable to different powertrain architectures and different component sizes. In addition to the DP [6, 31, 32], that finds the global solution recursively going backwards in time using Bellman's principle of optimality [3], local optimization methods have also been extensively used to find the global optimum. These methods can be used to find the optimum, by performing an offline optimization when the drive cycle is known, and they are also employed to design adaptive optimal strategies to achieve near optimal performances when the driving cycle is unknown. Much of the literature on local optimization methods pertain to PMP and/or ECMS [8, 27, 29].

The PMP [22] formulates and minimizes the Hamiltonian function (a function of the instantaneous cost and the state constraint) at each instant to obtain the optimal solution. PMP conditions, which in principles, are only necessary conditions of optimality in the case of Problem 12.1 become also sufficient.[1] This makes PMP a design tool to find the global optimal solution. Given Problem 12.1, PMP states that the optimal control solution $u^*(t)$ must satisfy the following conditions:

- $u^*(t)$ minimizes at each instant of time the Hamiltonian associated to the system:

$$H(u(t), SOC(t), \lambda(t)) = \lambda(t) \cdot \dot{SOC}(t) + \dot{m}_f(u(t))) \tag{12.12}$$

i.e.:

[1] Results from [13] and [14] prove the uniqueness of the solution of the optimal control problem under the satisfied assumption of constant battery efficiency over the SOC range of operation.

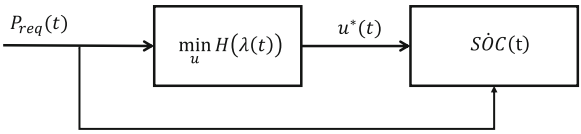

Fig. 12.3 Open-loop PMP-based energy management control scheme

$$u^*(t) = \min_{u \in \mathscr{U}} H(u(t), SOC(t), \lambda(t)) \tag{12.13}$$

$\mathscr{U}$ is the set of admissible solutions;

- the optimization variable $\lambda(t)$, also known as adjoint state or co-state must satisfy the dynamic equation along the optimal solution:

$$\dot{\lambda}(t) = -\left.\frac{\partial H}{\partial SOC}\right|_{u^*, SOC^*} \tag{12.14}$$

The optimal control sequence generated by (12.13) operates in open-loop as shown in Fig. 12.3.

Hence, the optimal solution u^* can only be obtained in simulation where the power request is known a-priori. In particular, the optimality of PMP resides in the perfect knowledge of the optimal co-state λ^* whose value varies from cycle to cycle. In [29] it is mathematically shown that the minimization of the Hamiltonian H is equivalent to the minimization of an equivalent fuel consumption function, used in the ECMS. ECMS, initially proposed by Paganelli et al. [21], is based on accounting for the use of stored electrical energy, in units of chemical fuel use (g/s), such that one can define an equivalent cost function taking into account the cost of electricity:

$$\dot{m}_{f,eq}(t) = s(t)\frac{E_{batt}}{Q_{lhv}} \cdot S\dot{O}C(t) + \dot{m}_f(t) \tag{12.15}$$

where E_{batt} is the battery energy and $s(t)$ is the *equivalent factor* that assigns a cost to the use of electricity, and the equivalent cost function $\dot{m}_{f,eq}(t)$ is equivalent to the Hamiltonian in PMP. If, on one hand, PMP/ECMS are practical tools to find the optimal solution to Problem 12.1 using a forward looking simulator, they can also been employed for real-time implementation.

In fact, the only control parameter in the PMP (or ECMS) is the co-state (or equivalent factor), which is cycle-dependent. The key idea to use the PMP (or ECMS) as a causal strategy resides in adapting the co-state as a function of driving conditions. From the PMP solution one can observe that the variation of the co-state as driving conditions change is correlated to the divergence of the actual SOC from its charge-sustaining reference value [20]. This observation has led to the development of an adaptation scheme based on feedback from SOC to be used in combination to the minimization of H [20]. The role of adaptation is to update the value of the co-state without using past driving information or prediction of future driving behavior, but

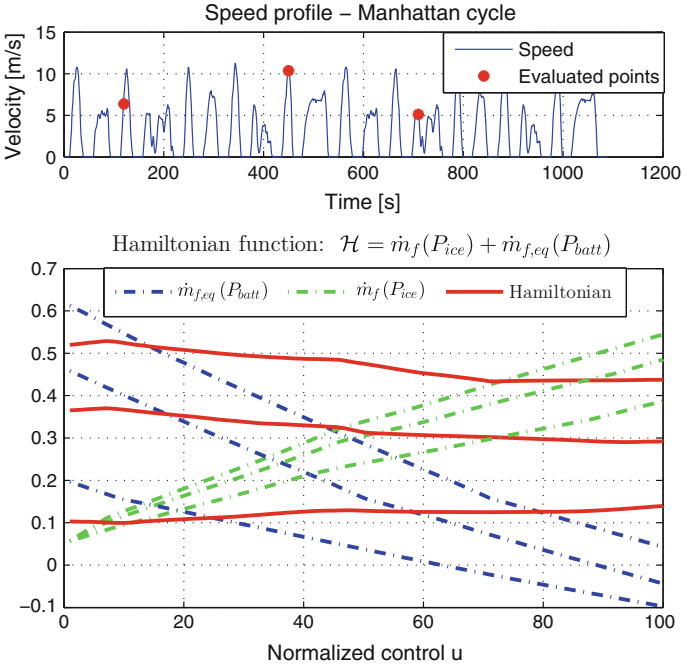

Fig. 12.4 Hamiltonian function H (*bottom*) evaluated for different instances of a Manhattan driving cycle (*top*) [19]

just using information of current SOC. For example, the adaptation can be performed via PI-like controller [15], or via an autoregressive moving average (ARMA) mechanism of the type [20]:

$$\lambda(k) = \frac{\lambda(k-1) - \lambda(k-2)}{2} + K \cdot (SOC_{ref} - SOC(k)) \tag{12.16}$$

which allows the adaptation to take place at regular intervals of duration T_s, ($t = kT_s, k = 1, 2, \ldots$), rather than at each time instant as in the case of PI-like based correction.

12.6 Motivation for Infinite-Time Horizon Optimization

The real-time controller based on A-PMP (12.16) requires the Hamiltonian function to be minimized instantaneously. This operation, that needs to be executed on-board at each tick of the clock, despite being computationally expensive, can lead in some cases to unpredictable no-optimal results, due to the fact that the Hamiltonian is in many instances of the driving cycle not a convex function of the control variable,

as one can see from Fig. 12.4. Different control values could be in principle equally suitable in the minimization process, leading to a not unique solution of the optimal control problem, thus causing undesirable chattering in the control outputs [26]. These issues have suggested to move towards a new research direction to find optimal solutions that would not have such a detrimental behaviour when used in a real-time setting. Inspired by Bernstein and Haddad's work [2, 11] on theoretical results on optimal nonlinear regulation problem involving non quadratic cost functionals, a first attempt to propose a new control framework for the energy management problem was done in [25]. The authors cast the energy management problem into a nonlinear optimal regulation problem where the battery SOC is optimally regulated to its reference target in the case of zero disturbance ($P_{req} = 0$). Preliminary results showed the feasibility of the closed-form control law in the simple case of vehicle at standstill and series hybrid architecture. Reduction in computational complexity and decreased sensitivity of the control parameter with respect to driving conditions were also showed. Nonetheless, two issues were not properly addressed in [25]: the stability definition and the extension of finite-time cost function into an infinite-time functional (needed to formally use the results from [2, 11]). In [19], a rigorous framework is developed where stability of the energy management state trajectory is finally defined while guaranteeing optimality by means of an analytical, cycle-independent control law. The novel framework is summarized in the next section and new simulation results comparing the performances of the new analitycal supervisory controller against PMP (used as a benchmark) and A-PMP (for on-line strategies comparison) are presented in Sect. 12.9.

12.7 From Finite-Time to Infinite-Time Horizon Optimal Control Problem

The energy management problem is reformulated as a nonlinear-nonquadratic infinite-time optimization problem. The new control framework consists in re-thinking the standard finite-time optimal control problem in HEV (Problem 12.1) as an infinite time horizon problem. To ensure optimality of vehicle operation when $t > T$, the $[0,\ T]$ optimization horizon is extended into the infinite horizon $[0,\ \infty]$, leading to a new cost function, J_∞ [19]:

$$J_\infty = \int_0^\infty \dot{m}_f(u(t)) \cdot g(t) dt \tag{12.17}$$

by means of the scalar positive function, $g(t)$:

$$g(t) = \frac{1 + \alpha \left(\frac{t}{T}\right)^q}{1 + \left(\frac{t}{T}\right)^q} \qquad 0 < \alpha < 1, \quad q > 0 \tag{12.18}$$

The role of the function $g(t)$ is to penalize the action of the control $u(t)$ for $t > T$ in order to approximate the finite-time cost J_T defined in (12.7) to the infinite-time functional (12.17). The system dynamics is reformulated in order to fit the problem in the form used in [11] (as discussed in [19]), where the nonlinear system is required to be dissipative with respect to a supply rate function.

12.7.1 System Dynamics Reformulation

In the new control framework, a Lyapunov-based approach is used to obtain a state-feedback control law to find the optimal torque/power split where the power requested (P_{req}) is regarded as a $\mathscr{L}_2$ disturbance. The battery state of energy (SOE), defined as the amount of battery energy stored at the present time ($E(t)$) to the maximum battery energy capacity (E_{max}), is used as state variable in this discussion. SOE is related to SOC by the following relationship [29]:

$$SOE(t) = SOC(t)\frac{V_L(t)}{V_{oc}^{max}} = \frac{E(t)}{E_{max}} \tag{12.19}$$

where V_L is the battery terminal voltage and V_{oc}^{max} the maximum open circuit voltage. Hence, the SOE dynamics:

$$\begin{cases} \dot{SOE} = -\eta_{batt}\dfrac{P_{batt}}{E_{max}} \\ E_{max} = Q_{max} \cdot V_{oc}^{max} \end{cases} \tag{12.20}$$

Defining $k = \frac{\eta_{batt}}{E_{max}\eta_{mot}}$, the battery SOE error $\zeta = SOE_{ref} - SOE$ is introduced, whose dynamics is described as a function of the control input (P_{ice}) and the disturbance (P_{req}) by virtue of Eq. (12.2):

$$\dot{\zeta} = -kP_{ice} + kP_{req} \tag{12.21}$$

Note that in parallel mode the power requested is the sum of accessory powers ($P_{accelec} + P_{accmecc}$) and the gearbox power (P_{gb}). When the vehicle is not moving ($v = 0$), instead, the power requested P_{req} only accounts for the accessory loads power. Thus, the disturbance power P_{req} is:

$$P_{req} = \begin{cases} P_{gb} + \eta_{mot} P_{accelec} + P_{accmecc} & v > 0 \quad \forall t \in [0,\ T] \\ \eta_{mot} P_{accelec} + P_{accmecc} & v = 0 \quad \forall t \in [T,\ \infty] \end{cases} \tag{12.22}$$

Consider an open set $\mathscr{Z} \subset \mathbb{R}$ such that $\zeta \in \mathscr{Z}$, a set $\mathscr{U} \subset \mathbb{R}$ such that $P_{ice} \in \mathscr{U}$, and a set $\mathscr{W} \subset \mathbb{R}$ such that $P_{req} \in \mathscr{W}$ and P_{req} in $\mathscr{L}_2$. The compact sets for the control, state and disturbance are:

$$\begin{cases} \mathscr{Z} = \left[SOE_{ref} - SOE_{max}, SOE_{ref} - SOE_{min}\right] \\ \mathscr{U} = \left[0, P_{ice}^{max}\right] \\ \mathscr{W} = \{P_{req} : P_{req} \in \mathscr{L}_2\} \end{cases} \tag{12.23}$$

Consider the following control system:

$$\begin{cases} \dot{\zeta} = -kP_{ice} + kP_{req}, \quad \zeta(0) = \zeta_0 \\ z = \zeta \end{cases} \tag{12.24}$$

where $\zeta = 0$ is an equilibrium point of the autonomous system and z is the performance output variable. Also consider the following functional cost [in virtue of (12.6)]:

$$J_\infty = \int_0^\infty \dot{m}_f(P_{ice}(t))dt = \int_0^\infty \frac{p_0(\omega_{ice}) + p_1(\omega_{ice}) \cdot P_{ice}(t)}{Q_{LHV}} dt \tag{12.25}$$

Problem 12.2 The **infinite-time optimal energy management problem** consists in minimizing the cost function (12.25) under system dynamics (12.24), with state and control variables lying in the compact sets $\mathscr{Z}$ and $\mathscr{U}$, and $P_{req} \in \mathscr{W}$.

Definition 12.1 Consider Problem 12.2 with $P_{req} \equiv 0$ and let $\phi(\zeta(t))$ be its optimal solution. Then the origin $\zeta(t) = 0$ of the closed-loop system under $\phi(\zeta(t))$ is asymptotically stable if $\zeta(t) \to 0$ for $t \to \infty$.

A typical SOC behavior obtained as a solution of Problem 12.2, is shown in Fig. 12.5. It can be noticed that the global constraint used in Problem 12.1 requiring $SOC(T)$ to be equal to the reference value SOC_{ref} is not met in this case as the convergence of SOC to SOC_{ref} is guaranteed only as $t \to \infty$.

12.8 Infinite-Time Nonlinear Optimal Control Strategy (NL-OCS)

With respect to the system (12.24) and the infinite cost function (12.25) [11] defines the Hamiltonian function H as following:

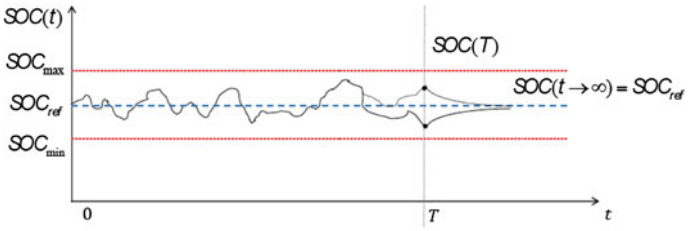

Fig. 12.5 Typical SOC profile as a solution of a infinite-time optimization problem including stability

$$H(\zeta, P_{ice}, \lambda) = \dot{m}_f(P_{ice}) + \Gamma(\zeta, P_{ice}) + \lambda \cdot (k P_{ice}) \tag{12.26}$$

where $\Gamma(\zeta, P_{ice})$ is a positive scalar function (to be selected), and λ is the co-state variable. In order to have the Hamiltonian function zero at the minimum value, as requested in [11], a shifting of the H is operated as follows:

$$\bar{H}(\zeta, P_{ice}, \lambda) = H(\zeta, P_{ice}, \lambda) - p_0(\omega_{ice}) \tag{12.27}$$

Theorem 12.1 *Consider the system (12.24) with functional cost (12.25). Then, the feedback control law $P^*_{ice}(\zeta)$ defined as:*

$$P^*_{ice} = \phi(\zeta) = \begin{cases} \frac{2k^2(\mu^4\zeta^3)^2}{(k\mu^4\zeta^3 - p_1(\omega_{ice})\ g(t))\gamma^2} & \zeta > \bar{\zeta} \vee \zeta \leq 0 \\ \zeta^2 & 0 < \zeta \leq \bar{\zeta} \end{cases} \tag{12.28}$$

with $\bar{\zeta} = \left(\frac{p_1(\omega_{ice})}{k\mu^4}\right)^{\frac{1}{3}}$, *is such that:*

1. *the solution $\zeta(t) = 0, t \geq 0$ of the closed-loop system is locally asymptotically stable in accordance to Definition 12.1.*
2. *the adjoint performance functional $\mathscr{J}(\zeta, P_{ice}(\zeta))$*

$$\mathscr{J}(\zeta, P_{ice}) = \int_0^\infty \left[\dot{m}_f(P_{ice}) + \Gamma(\zeta, P_{ice})\right] dt \tag{12.29}$$

is minimized.

Proof Consider the candidate Lyapunov function

$$V(\zeta) = \frac{1}{4}\mu^4\zeta^4, \quad \mu > 0 \in R \tag{12.30}$$

then we can define the storage function $\Gamma(\zeta, P_{ice})$ and the supply rate function $r(\zeta, P_{req})$, associated to the system (12.24) and the Lyapunov function (12.30), as:

$$\begin{cases} \Gamma(\zeta, P_{ice}) = \dfrac{1}{\gamma^2}\left(\dfrac{\partial V}{\partial \zeta}\right)^2 k^2 \cdot \left(1 + \log(P_{ice}^2)\right) \\ r(\zeta, P_{req}) = \gamma^2 P_{req}^2 - \zeta^2 \end{cases} \tag{12.31}$$

The proof of Theorem 12.1, following the same reasoning provided in [11], is based on a series of sufficient conditions that ensure optimality and stability that are shown to hold true when the optimal feedback control $\phi(\zeta) = P_{ice}^*(\zeta)$ is used.

1. The Lyapunov function $V(\zeta)$ assumes its minimum value of 0 at the origin.

$$V(0) = 0 \tag{12.32}$$

2. $V(\zeta)$ is a positive definite function because it is a quadratic scalar function with the minimum at the origin.
3. The optimal feedback control law is zero at the origin, i.e., from (12.28):

$$P_{ice}^*(0) = 0 \tag{12.33}$$

4. The optimal control law (12.28) makes the origin $\zeta(t) = 0$ asymptotically stable when $P_{req} = 0$, equivalently:

$$\frac{\partial V}{\partial \zeta} \cdot k P_{ice}^*(\zeta) < 0, \quad \zeta \neq 0 \tag{12.34}$$

In order to show (12.34), without loss of generality we consider P_{batt} as new control variable with $P_{req} = 0$. Thus:

$$P_{batt}^* = \begin{cases} -\frac{2k^2(\mu^4\zeta^3)^2}{(k\mu^4\zeta^3 - n_1(\omega_{mot})\ g(t))\gamma^2} & \zeta > \bar{\zeta}^* \vee \zeta \leq 0 \\ -\zeta^2 & 0 < \zeta \leq \bar{\zeta}^* \end{cases} \tag{12.35}$$

where $\bar{\zeta}^* = \left(-\dfrac{n_1(\omega_{mot})}{k\mu^4}\right)^{\frac{1}{3}}$, and this makes (12.34) become:

$$\mu^4 \cdot \zeta^3 \cdot k \cdot k P_{batt}^*(\zeta) < 0, \quad \zeta \neq 0 \tag{12.36}$$

In the domain $0 < \zeta \leq \bar{\zeta}^*$, it is immediate to see that

$$-\mu^4\ \zeta^3\ k\ \zeta^2 < 0 \tag{12.37}$$

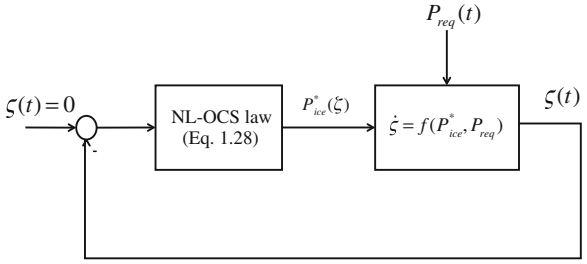

Fig. 12.6 Closed-loop energy management control scheme based on the analytical NL-OCL solution

In the domain $\zeta > \bar{\zeta}^* \vee \zeta \leq 0$ denominator of (12.36) is positive when ζ is positive and negative otherwise, thus leading to:

$$\begin{cases} -\mu^4\zeta^3 k \cdot 2k^2(\mu^4\zeta^3)^2 < 0 & \zeta > \bar{\zeta}^* \\ \mu^4\zeta^3 k \cdot 2k^2(\mu^4\zeta^3)^2 < 0 & \zeta \leq 0 \end{cases} \tag{12.38}$$

5. The Hamiltonian function (12.27) takes on the minimum value when the optimal control law (12.28) is applied. The shifted hamiltonian $\bar{H}$,

$$\bar{H}\left(\zeta, P^*_{ice}, \frac{\partial V}{\partial \zeta}\right) = \dot{m}_f + \Gamma(\zeta, P^*_{ice}) + \frac{\partial V}{\partial \zeta} k P^*_{ice}(\zeta) \tag{12.39}$$

becomes

$$\bar{H} = p_1\, P_{ice} + \frac{1}{\gamma^2} k^2 \left(\mu^4\zeta^3\right)^2 \left(1 + \log(P^2_{ice})\right)^2 + \mu^4\zeta^3 k P_{ice} \tag{12.40}$$

for the system (12.24) and cost function (12.25). It can be easily shown that the closed-loop controller (12.28) is a minimum of the $\bar{H}$ (the stationary first order conditions and the second order convexity conditions are verified).
6. The passivity condition with respect to the disturbance input P_{req} requires that the following inequality is satisfied:

$$\left(\frac{\partial V}{\partial \zeta}\right) \cdot k \cdot P_{req} \leq r(\zeta, P_{req}) + \dot{m}_f + \Gamma(\zeta, P^*_{ice}) \tag{12.41}$$

A second order algebraic inequality in P_{req} is obtained which is verified when $\gamma \leq \bar{\gamma} = 2.369$. *Q.D.E.*

In virtue of Theorem 12.1, the origin $\zeta = 0$ of the closed-loop system is optimally locally asymptotically stable when $P_{req} = 0$. Moreover, P^*_{ice} is optimal with respect to the adjoint functional $\mathscr{J}(\zeta, P_{ice}(\cdot))$, which is an upper bound for J_∞.

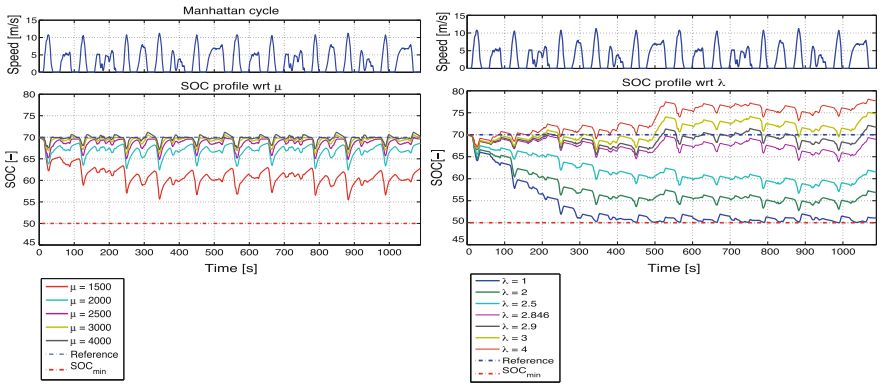

Fig. 12.7 SOC trajectories from: (1) NL-OCS as μ varies (*left*) and (2) PMP as λ varies (*right*) for the Manhattan driving cycle

The optimal control law obtained from Theorem 12.1 is referred to as Nonlinear Optimal Control Strategy (NL-OCS) and it is implemented according to the closed-loop system scheme shown in Fig. 12.6. To the best knowledge of the author of this article, this is the first time that an analytical supervisory controller is proposed to solve the energy management problem in HEVs. In the optimal control law (12.28) that operates from SOC feedback, the values of k, $p_1(\omega_{ice})$ are known from the vehicle models, γ is a constant whose upper bound was obtained from the theorem's proof, and μ is the only calibration parameter that needs to be selected for on-board implementation.

12.9 Strategies Comparison: Simulation Results

In this section, we first evaluate the novel closed-loop supervisory controller against the benchmark solution from PMP and then we compare the NL-OCS against the real-time implementable A-PMP to show the effectiveness of the proposed control-law for on-board implementation. Offline simulations are performed to test the sensitivity of the new model-based strategy against the calibration parameter μ. Results are shown on the left plot of Fig. 12.7 where different SOC profiles from NL-OCS are shown for different value of μ. On the left plot of Fig. 12.8 the fuel consumption (FC) is plotted together with $\Delta SOC = SOC(T) - SOC(0)$ (for different driving cycles) to measure the ability of the control law to guarantee charge-sustainability. On the right hand side of Fig. 12.7 and Fig. 12.8 we show: (1) the solution obtained from PMP for different values of the co-state λ and, (2) the high sensitivity of charge-sustainability to the co-state λ.

It is well known, in fact, that performance of PMP is highly dependent on the co-state λ, both in terms of charge-sustainability and fuel consumption (see, for instance

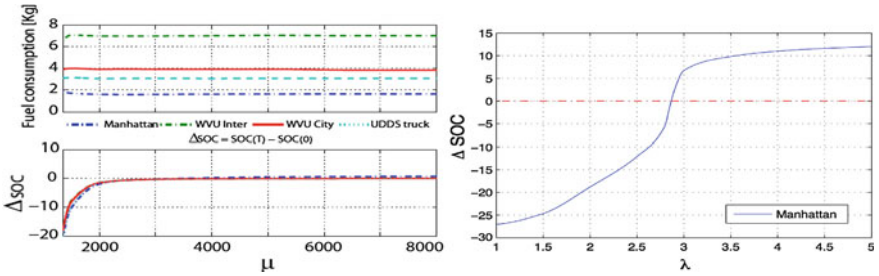

Fig. 12.8 NL-OCS: fuel consumption and $\Delta SOC = SOC(T) - SOC(0)$ as a function of μ for four different driving cycles (*left*). PMP: ΔSOC as a function of λ for Manhattan driving cycle (*right*)

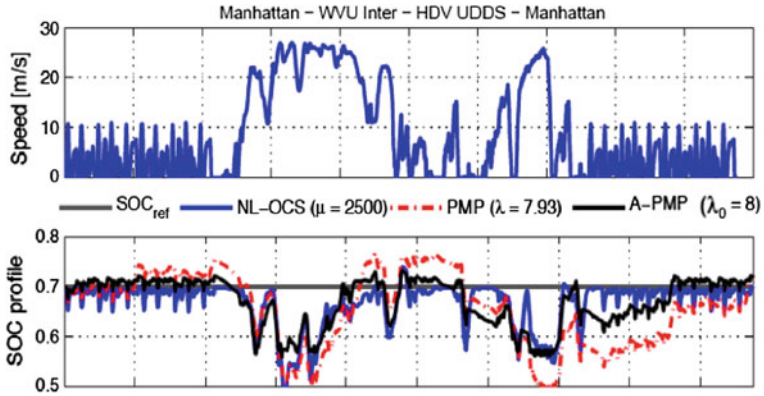

Fig. 12.9 SOC profiles from PMP, NL-OCS and A-PMP

[28]). The results of this analysis are used to calibrate the NL-OCS for on-board implementation. A combined driving cycle obtained by concatenating a Manhattan, West Virginia Urban (WVU) Interstate, Heavy-Duty UDDS, and Manhattan driving cycles is used to validate and compare the NL-OCS against the PMP solution and the real-time controller A-PMP. The three SOC profiles are shown in Fig. 12.9 and a quantitative analysis in terms of fuel economy and engine efficiency of the three control strategies is reported in Table 12.2. Not only does the analytical control law guarantee optimality (with values within 1 % from the PMP benchmark solution) for a wide range of values of the control parameter μ (see, Fig. 12.8), but also it guarantees low sensitivity against driving characteristics, making the performance of the new strategy driving cycle independent. In addition, the calibrated NL-OCS also shows better performance in terms of fuel consumption than the real-time A-PMP. Above all, the main advantage of having an analytical solution is in the fast execution of the control action as opposed to the computational burden required by the instantaneous minimization operation of A-PMP. In [19], it is reported that the NL-OCS solution is up to 5 times faster than the A-PMP. The NL-OCS can be implemented in the

Table 12.2 Fuel consumption and engine efficiency comparison between the PMP, A-PMP and NL-OCS solutions

Controller	FC m_f (kg)	Norm. fuel cons. %	ICE eff.
PMP	13.11	100	0.319
A-PMP	13.36 ($< 2\,\%$)	98.13	0.309
NL-OCS	13.24 ($< 1\,\%$)	99.02	0.310

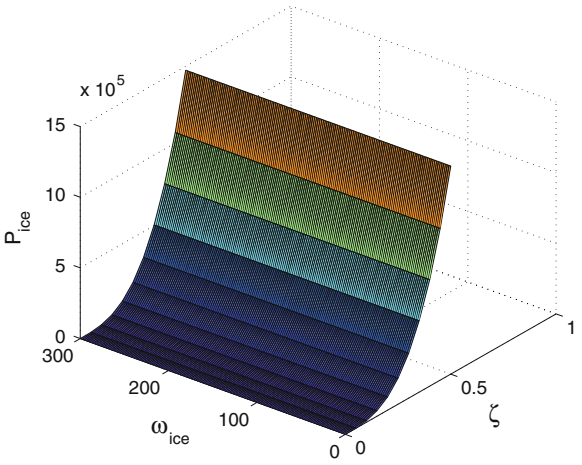

Fig. 12.10 Engine power map: $P_{ice} = f(\omega_{ice}, \zeta)$

form of a look-up table, by mapping the power issued by the control law (12.28) as a function of ζ and the engine speed ω_{ice}, as shown in Fig. 12.10.

12.10 Conclusions

In this chapter, we have first presented the standard formulation of the energy management problem in HEVs and reviewed the PMP and A-PMP methods. As a real-time implementable strategy, if on one hand the A-PMP is very promising as it performs near to the global optimum, on the other hand, the high computational burden due to the instantaneous minimization can make the use of this strategy prohibitive for in vehicle operation. A new framework centered around the theory of nonlinear, nonquadratic optimal control has been developed and presented in this chapter. An analytical, cycle-independent, state-feedback supervisory controller has been proposed that achieves optimality with respect to an infinite time horizon performance functional while guaranteeing asymptotic stability. The proposed control law was implemented in a pre-transmission parallel hybrid heavy-duty vehicle and the performances of the closed-loop system were compared to the benchmark solution

provided by the PMP and the real-time solution provided by A-PMP. The advantages offered by the newly designed solutions are: (1) low calibration effort (only one parameter needs to be calibrated); (2) low sensitivity to the control parameter; (3) fast execution for on-board applications; (4) close-to-the-optimum performance despite the driving mission.

Acknowledgments The author would like to deeply thank Roberto Mura for taking this research a step forward, Lorenzo Serrao for the enjoyable and productive discussions, Yann Guezennec, Giorgio Rizzoni, and Stephen Yuorkovich for the productive iterations.

References

1. Argonne National Laboratory: Powertrain system analysis toolkit (PSAT) documentation. DuPage County, IL, http://web.anl.gov/techtransfer/pdf/PSAT.pdf
2. Bernstein DS (1993) Non quadratic cost and nonlinear feedback control. Int J Robust Nonlinear Control 3:211–229
3. Bertsekas DP (1995) Dynamic programming and optimal control. Athena Scientific, Belmont
4. Bianchi D, Rolando L, Serrao L, Onori S, Rizzoni G, Al-Khayat N, Hsieh TM, Kang P (2011) Layered control strategies for hybrid electric vehicles based on optimal control. Int J Electric Hybrid Veh 3:191–217
5. Biasini R, Onori S, Rizzoni G (2013) A rule-based energy management strategy for hybrid medium duty truck. Int J Powertrains 2(2/3):232–261
6. Brahma A, Guezennec Y, Rizzoni G (2000) Optimal energy management in series hybrid electric vehicles. In: Proceedings of the 2000 American control conference, vol 1, issue 6, pp 60–64.
7. Chan CC (2002) The state of the art of electric and hybrid vehicles. Proc IEEE 90(2):247–275
8. Cipollone R, Sciarretta A (2006) Analysis of the potential performance of a combined hybrid vehicle with optimal supervisory control. In: Proceedings of the 2006 IEEE international conference on control applications, pp 2802–2807.
9. Ebbesen S, Elbert P, Guzzella L (2012) Battery state-of-health perceptive energy management for hybrid electric vehicles. IEEE Trans Veh Technol 61(7):2893–2900
10. Guzzella L, Sciarretta A (2007) Vehicle propulsion systems: introduction to modeling and optimization, 2nd edn. Springer, Berlin
11. Haddad WM, Chellaboina V (2008) Nonlinear dynamical systems and control: a lyapunov-based approach. Princeton University Press, NJ
12. Johnson VH, Wipke KB, Rausen DJ (2000) HEV control strategy for real-time optimization of fuel economy and emissions. SAE Paper number No. 2000–01-1543.
13. Kim N, Cha S, Peng H (2011) Optimal control of hybrid electric vehicles based on Pontryagin's minimum principle. IEEE Trans Control Systems Technol 19(5):1279–1287
14. Kim N, Rousseau A (2012) Sufficient conditions of optimal control based on Pontryagin's minimum principle for use in hybrid electric vehicles. Proc Inst Mech Eng, Part D: J Automobile Eng 226:1160–1170
15. Koot M, Kessels J, de Jager B, Heemels W, van den Bosh PPJ, Steinbuch M (2005) Energy management strategies for vehicular electric systems. IEEE Trans Veh Technol 54(3):771–782
16. Lin CC, Peng H, Grizzle JW, Kang JM (2003) Power management strategy for a parallel hybrid electric truck. IEEE Trans Control Syst Technol 11(6):839–849
17. Mi C, Masrur MA, Gao DW (2011) Hybrid electric vehicles: principles and applications with practical perspectives. Wiley, New York
18. Miller JM (2003) Propulsion systems for hybrid vehicles. The Institution of Electrical Engineers, London

19. Mura R, Utkin V, Onori S (2013) Ecasting the HEV energy management problem into an infinite-time optimization problem including stability. In: 52nd IEEE CDC.
20. Onori S, Serrao L, Rizzoni G (2010) Adaptive equivalent consumption minimization strategy for hybrid electric vehicles. In: Proceedings of the 2010 ASME DSCC, pp 499–505.
21. Paganelli G, Ercole G, Brahma A, Guezennec Y, Rizzoni G (2001) General supervisory control policy for the energy optimization of charge-sustaining hybrid electric vehicles. JSAE Rev 22:511–518
22. Pontryagin L, Boltyanskii VG, Gamkrelidze RV, Mishchenko EF (1962) The mathematical theory of optimal processes. Wiley, NJ
23. Rizzoni G, Peng H (2013) Hybrid and electric vehicles: the role of dynamics and control. In: ASME dynamic systems and control magazine, pp 10–17.
24. Sampathnarayanan B (2013) Analysis and design of stable and optimal energy management strategies for hybrid electric vehicles. Ph.D. Dissertation The Ohio State University.
25. Sampathnarayanan B, Onori S, Yurkovich S (2012) An optimal regulation strategy for energy management of hybrid electric vehicles. In: 51st IEEE CDC.
26. Sciarretta A, Back M, Guzzella L (2004) Optimal control of parallel hybrid electric vehicles. IEEE Trans Control Syst Technol 12:352–363
27. Sciarretta A, Guzzella L (2007) Control of hybrid electric vehicles. IEEE Control Syst Mag 27:60–70
28. Serrao L, Onori S, Rizzoni G (2011) A comparative analysis of energy management strategies for hybrid electric vehicles. ASME JDSMC 133(3):1–9
29. Serrao L, Onori S, Rizzoni G (2009) ECMS as a realization of Pontryagin's minimum principle for HEV control. In: Proceedings of the 2009 American control conference, pp 3964–3969.
30. Serrao L, Onori S, Sciarretta A, Guezennec Y, Rizzoni G (2011) Optimal energy management of hybrid electric vehicles including battery aging. In: Proceedings of the 2011 American control conference, pp 2125–2130.
31. Sundstrom O, Guzzella L (2009) TA generic dynamic programming Matlab function. In: Control applications (CCA) intelligent control (ISIC), 2009 IEEE, pp 1625–1630.
32. Sundstrom O, Guzzella L, Soltic P (2008) Optimal hybridization in two parallel hybrid electric vehicles using dynamic programming. In: Proceedings of the 17th IFAC world congress.